



## 1 Introduction

Catchment hydrology and water resources is driven by climate, and strongly modulated by human activities. Climate variability affects catchment runoff chiefly through precipitation and potential evaporation variability (Scanlon et al., 2007; Huicheng et al., 2013; Ward et al., 2009; Chang et al., 2010). Human activities include land use/cover change, reservoir operations, and direct water extraction from surface-water and groundwater, all of which can alter river runoff. It is important to separate and quantify the effects of climate variability/climate change so that it can be used for land use planning, water extraction and water resources management. With increasing scarcity of water resources, hydrologists and decision and policy makers have paid considerable attention to how much of the observed change in annual runoff can be attributed to climate variability and human activities (Zhang et al., 2008; Tomer and Schilling, 2009; Roderick and Farquhar, 2011; Destouni et al., 2013).

Catchment experiments to determine the influence of vegetation change on water balance are very useful, however are often limited to small scales. A number of catchment afforestation and deforestation studies have been conducted. Most of the results indicate that catchment runoff is significantly decreased after afforestation and increased after deforestation (Van Lill et al., 1980; Zhang et al., 2001; Tuteja et al., 2007). Two other main approaches, process-based and statistic based, have generally been used. The process-based method by using hydrological models quantify the contribution of climate variability to runoff change by varying the meteorological inputs for fixed land use/cover conditions (Xu et al., 2013; Petchprayoon et al., 2010; Lin et al., 2010; Tesfa et al., 2014). However the results of hydrological model studies have numerous uncertainties caused by the model structure, parameter calibration, and scale issues. Statistical methods for identifying the contributions of climate and human impacts on runoff have also been used especially in regions where long-term climate and hydrologic data are available (Hamed, 2008; Notebaert et al., 2011; Renner et al., 2012; Roudier et al., 2014). Among the statistical methods, streamflow elasticity

5253

has been commonly used to quantify the influence of changes in precipitation and potential evapotranspiration on streamflow (Sankarasubramanian et al., 2001; Chiew, 2006; Fu et al., 2007; Roderick and Farquhar, 2011). Streamflow elasticity can be obtained non-parametrically from observations or employing a parametric model, such as the Budyko hypothesis or other models. The Budyko hypothesis has been widely used to evaluate the impact of climatic variables on runoff as it is an easy method with limited requirement of climate data (Donohue et al., 2007; Liu et al., 2009; Wang et al., 2011, 2013).

Climate change and human activities have had tremendous impacts on water resources of China's highly urbanized regions. One such river basin is the Jinghe River, which is the secondary tributary of the Yellow River, the largest tributary of the Weihe river in China with an area of 45 400 km<sup>2</sup> and average annual natural runoff of 12.3 × 10<sup>9</sup> m<sup>3</sup>. This is an important watershed of Shaanxi Province that supplies drinking water for a population of over 6 million. The area has been an important economic center of Shaanxi province in China and water shortage became a bottleneck for economic progress. Human activities have become extensive in the Jinghe River during the last several decades such as water withdrawal, soil and water conservation project. Climate change studies in the Yellow River basin (YRB) have reported warming trends at a rate of 1.28 °C (50 years)<sup>-1</sup>, while the average precipitation dropped about 8.8% over the second half of the 20th century. Combination of these effects reduced runoff (Gao et al., 2013; Chang et al., 2014). Few studies were devoted to analyze the contribution of climate variability and human activity to runoff variation in the Jinghe River basin. However, such topic has attracted attentions and interests of local water managers and government.

The aim of this study is to investigate the impacts of climate variability and human activity on streamflow using the concept of streamflow elasticity and two process-based hydrologic models, TOPMODEL and VIC, that are fundamentally different in the representation of runoff generation. The Jinghe River Basin (JRB) is chosen as the study area, which presents a significantly decreasing trend of annual streamflow

5254

since 1990. This paper is arranged as follows: Sect. 2 describes the study area and data sources; Sect. 3 is devoted to the methods used; Sect. 4 provides hydrological modelling and elasticity method results and discussion; Sect. 5 compares the results from hydrological modelling with the elasticity-based method; and Sect. 6 several conclusions generated from the present study are discussed.

## 2 Study area and data

The Jinghe river basin (JRB) ( $106^{\circ}14' \sim 108^{\circ}42' \text{ E}$ – $34^{\circ}46' \sim 37^{\circ}19' \text{ N}$ ) located in semi-arid area in China is about 455 km long with a drainage area of 45 400 km<sup>2</sup> (Fig. 1). The climate is temperate, with cool, dry winters and hot summers, and the mean annual temperature is in the 7.8–13.5 °C range across the basin. Mean annual precipitation is about 514 mm, 80 % of which falls between June and October, and mean annual areal potential evapotranspiration is 870 mm. Both precipitation and runoff have strong inter-annual and intra-annual variability. The seasonal variation of runoff is similar to that of precipitation. The runoff between July and October is approximately 65 % of the mean annual runoff. Zhangjiashan station is the most downstream hydrometric station on the Jinghe River main stream.

Human activities have become extensive in the JRB during the last several decades. Water withdrawal has been increasing rapidly due to the increase of population, industry and agricultural water demand. Thick and highly erodible loess, unevenly distributed rainfall, and relatively high intensity of rainstorms, lead to high soil loss rates across the basin. To reduce soil loss, soil and water conservation measures have been undertaken since the 1970s, which resulted in increase in vegetation cover. Therefore, climate variability combined with human activities has contributed to the decrease of the streamflow in the JRB.

In our analysis daily, monthly, and annual climate variables and observed runoff are used. Daily meteorological data, including precipitation, air temperature (mean, maximum, and minimum air temperature), sunshine hours, relative humidity, and

5255

wind speed, were collected from ten stations during 196–2010 from the China Meteorological Administration (CMA). Catchment information data set, including catchment boundary and runoff ratio, was from the Ministry of Water Resources (MWR) of the People's Republic of China. The monthly and annual precipitation was then established from the collected data. Air temperature data were prepared by calculating monthly mean and annual maximum, minimum, and mean air temperature values from daily data. The monthly evaporation was calculated using the monthly wind speed, sunshine hours, relative humidity and air temperature using the FAO recommended Penman–Monteith P-M method. The daily streamflow data were gathered for the same period for Zhangjiashan hydrological station from the Shaanxi Hydrometric and Water Resource Bureau. The DEM data were obtained from the SRTM 40 m Digital Elevation Data. The soil data were extracted from the FAO two-layer 5 min 16-category global soil texture maps. Figure 2 shows the location of the meteorological stations and hydrological station in the basin.

## 3 Methodology

### 3.1 Framework of analysis

The historic streamflow series can be split into subseries from a year before which human activity is negligible. The record years prior to this break year are defined as baseline period, while the record years after this break year are defined as changed period. The difference between the mean annual streamflow during changed period ( $Q_2$ ) and the mean annual streamflow during baseline period ( $Q_1$ ) can represent the total change of streamflow ( $\Delta Q$ ) after the break year. The  $\Delta Q$  can be regarded as a function of climatic variables and integrated effects of topography, soil, land use/land cover and human activities like water withdrawing. Under the assumption that topography and soil of the study area did not vary during the study period,  $\Delta Q$  could be referred to a combination of climate variability and human activity, and can be estimated

5256



### 3.3 Modeling-based approach for $\Delta Q_C$ or $\Delta Q_H$

Hydrological models can also be used to assess the impacts of climate change on streamflow. A hydrologic model was calibrated and validated using data during baseline period, to estimate  $\Delta Q_C$  or  $\Delta Q_H$ . The model was run using climate (e.g., precipitation and temperature) during changed period with human activity (i.e., land use and management) and during the baseline period.  $\Delta Q_C$  is estimated as the difference of the mean annual average of simulated streamflow during changed period than the mean annual average of simulated streamflow during baseline period, whereas,  $\Delta Q_H$  is estimated as the difference of the mean annual average of simulated streamflow during changed period than the mean annual average of observed streamflow during changed period.

TOPMODEL (Beven and Kirkby, 1979) is a semi-distributed variable contributing area hydrological model. It is based on simple physical reasoning and assumes that there is a steady transfer of water in the saturated zone along hillslopes, with a water table nearly parallel to the ground surface. It considers two stream flow sources: (shallow) groundwater and saturation overland flow. The model assumes an exponential decay of soil transmissivity with increasing water table depth and considers two main parameters for the dynamics of the saturated store: the recession parameter  $m$  [L] and the average soil transmissivity at saturation  $T$  [ $L T^{-1}$ ]. The classical form for the topographic index that follows from the exponential assumption,  $\lambda_i = \ln(a/\tan b)$  was used, where  $a$  is the drained area per unit length of contour curve, and  $b$  is the topographic gradient. All points in the catchment with the same topographic index are predicted as having the same deficit, i.e. they are considered as hydrologically similar. Since the early 1990s, TOPMODEL has been widely applied to watersheds all over the world because it can provide spatially distributed hydrologic information with available input requirements (e.g., Digital Elevation Model (DEM) data) (Seibert et al., 1997; Chen and Wu, 2012; Furusho et al., 2013). Also, some papers have applied the TOPMODEL in semi-arid area basin, such as the Yellow River in China, and the results show that this model

5259

is applicable in a wide range of environments (Xiong et al., 2004; Boston et al., 2004; Gumindoga et al., 2015).

The VIC model is a large-scale hydrologic model, originally developed at the University of Washington (Liang et al., 1994; Grimson et al., 2013; Gao et al., 2011). The hydrological processes of the model includes interaction of the atmosphere with underlying vegetation and soils, where the dynamic water and energy fluxes are considered. One distinguishing characteristic of the VIC model is that it represents the sub-grid spatial heterogeneity of precipitation with sub-grid spatial variability of soil infiltration capacity. A variable infiltration curve (Xinjiang model citation) is used to represent the sub-grid variability of soil infiltration capability under different land cover and soil types. Three types of evaporation are considered in the model: evaporation from the canopy layer of each vegetation class, transpiration from each of the vegetation classes, and bare soil evaporation. VIC model has been successfully applied to assess the impact of climate change on hydrology and water resources in China (Wang et al., 2010; Bao et al., 2012; Su and Xie, 2003).

## 4 Results and discussion

### 4.1 The analysis of streamflow, precipitation, evaporation and temperature

The regional average precipitation, potential evaporation and temperature in the JRB during 1960–2010 was calculated by using the Tyson polygon method of the ArcGIS 9.3 according to the corresponding data of ten hydrometeorology stations.

Both the annual observed precipitation in the JRB and streamflow at Zhangjiashan station showed a statistically decreasing trend (Fig. 3), while the streamflow had a larger decrease. The values of the regression slope were respectively  $-1.44$  and  $-0.58$ . The annual mean value of runoff was  $43.47$  mm from 1960 to 1990, and reduced by  $17.39\%$  compared with the multi-year average streamflow. The average annual streamflow was  $27.05$  mm during 1991–2010 reduced by  $-26.96\%$ , therefore, the

5260

speed of streamflow decrease was higher since 1990. The three-year moving curve showed that precipitation and streamflow fluctuation was similar, which indicated that precipitation was the main source of streamflow. The statistical results of precipitation, streamflow and runoff coefficient in JRB were listed in Table 1. The maximum of precipitation and streamflow appeared in the same time of 1964, however the minimum occurred in different years which resulted from water withdrawal and other reasons such as changes in underground water. The precipitation and streamflow during flood season (from July to October) accounted for 64.21 and 59.17 %, respectively, and the proportion of dry period (from November to March of next year) was 6.15 and 17.57 %, respectively. The proportion of rainfall that becomes runoff is low, with a mean annual runoff ratio of 0.07, but increases during wet years.

The result of Mann–Kendall's test showed the same decreasing trend for annual precipitation and streamflow in JRB from 1960 to 2010. The  $Z$  value of streamflow and precipitation was respectively  $-4.26$  and  $-1.39$  at confident level of 99 and 90 %, which means the significant decreasing trend for streamflow and insignificant for precipitation at  $\alpha = 0.05$  level.

Table 2 showed the monthly and seasonally potential evaporation and temperature in the JRB, which indicated that the evaporation (122 mm) and temperature ( $20.7^{\circ}\text{C}$ ) in summer are much higher than other three seasons, and the maximum value of evaporation and temperature appeared in June and July respectively. The inter-annual variation and characteristic values of evaporation and temperature were shown in Fig. 4 and Table 3. The mean annual evaporation in 80s (822 mm) has decreased compared with 60s values (861 mm), and started to grow slowly in 90s (973 mm). Temperature value showed a slight upward trend in the 70s, 80s, and had a sharp upward trend in the 90s era. The  $Z$  value of evaporation and temperature for Mann–Kendall's test were 0.4 and 4.12 respectively, which means evaporation presents an insignificant increasing trend, but the temperature has a significant increasing trend.

5261

## 4.2 Hydrological model calibration and validation

In this study, two hydrological models, TOPMODEL and VIC model, are used to investigate the effects of climate variability and human activity on streamflow. The original TOPMODEL has four parameters, i.e. the maximum allowable root storage deficit ( $SR_{\max}$ ), the transmissivity of the soil in saturated state ( $T$ ), the maximum moisture max deficit ( $S_{zm}$ ), and the recharger delay parameter ( $T_d$ ). There are six parameters we used in the calibration of the VIC model. These include three baseflow parameters:  $D_m$ ,  $W_s$ , and  $D_s$ ; the variable soil moisture capacity curve parameter:  $b$ ; and two parameters,  $d_2$  and  $d_3$ , that controls the thickness of the second and third soil layer, respectively. There was little human activity in the JRB prior to 1970, so we have taken 1960–1970 as the baseline period for this study. The models were calibrated using the historical data from 1960 to 1966 and validated against the observation during the period of 1967–1970. During the calibration, adjustments were made to minimize the sum of squares of the difference between the modelled and recorded monthly streamflows. Nash–Sutcliffe efficiency coefficients (NSE) and relative Water Balance Error percentage (WBE) were used for the model assessment using observed data and model estimates.

During model simulation, the digital elevation quadrangles at 40 m resolution with study area was used (Fig. 5). In the TOPMODEL, several sub-basins were divided according to the flow accumulation by means of ArcGIS, and the flow direction, flow accumulation were extracted in ARCGIS to calculate the topographic index-area ratio of sub-basin. Monthly precipitation, potential evapotranspiration and observed streamflow acted as input data. Figure 6 shows simulated and recorded streamflow for the calibration and validation period. A calibrated VIC model was also employed to separate hydrological impacts of land use change and climate change. The VIC model was used for streamflow simulation at a  $0.5^{\circ}$  spatial and daily temporal resolution in the JRB (Fig. 5). Figure 6 shows simulated and observed streamflow for the calibration and validation period with outputs computed on a monthly basis.

5262

In the scatter plots in Fig. 7 the observed monthly streamflow was plotted along the  $x$  axis and the model simulated streamflow (calibration and validation) were plotted along the  $y$  axis. The scatter plots in Fig. 7 showed that both the hydrological models performed reasonably well in model calibration with high NSE values and low WBE values. The correlation of simulated streamflow and measured streamflow was higher in calibration period,  $R$  value exceeds 0.8. The observed and simulated streamflow over the non-calibration period was compared to determine the suitability of the model for this study. The validation NSE and WBE values (see Fig. 7) suggested that both the rainfall–runoff models and the calibration method used in this study are robust for the calibrated model to be used over an independent simulation period adequately. Also, the results justified the suitability of the models applied for assessing the change in streamflow due to climate variability and human activity.

### 4.3 Hydrological model simulation results

The calibrated model parameters for both the models from baseline periods of 1960 to 1970 were used with the meteorological time series to simulate streamflow for the changed period of 1971–2010, and to investigate the effects of climate variability and human activity. The scatter plots in Figs. 8 and 9 showed the comparison of the simulated and observed monthly and annual streamflows time series for the JRB for the entire modelling period (1971–2010) for the TOPMODEL and VIC model respectively.

The model simulation results showed that streamflow had a strong response to the environment change after 1970. In the scatter plots in Fig. 8, the simulated monthly streamflow values were mostly above the 1 : 1 line indicating that the simulated streamflow was much higher than the observed streamflow for most of the months. The time series plots in Fig. 9 showed that the simulated annual runoff values were always higher than the observed streamflow. The effect of climate variability has been eliminated from the simulations for the changed periods by using the actual observed climate to drive the calibrated models. The difference in observed and simulated streamflow during the changed period is due to the difference in land cover and other

5263

human activities. The results indicated that human activity has caused significant reduction in streamflow, and these results were consistent with the finding (Chang et al., 2014; Tang et al., 2013; Zhan et al., 2014).

### 4.4 Influence of human activity and climate variability

To separate and quantify the effects of human activity on streamflow after 1970, the simulated streamflow for the two models were compared against the observed values during baseline and changed period (methodology details in Sect. 3.1). The differences in observed streamflow values during baseline period and changed periods are caused by the differences in climatic conditions and human activity. Tables 4 and 5 summarized the mean annual statistics of observed and simulated streamflows for different periods of 1970s, 1980s, 1990s and 2000s. The third column provided the values for  $\Delta Q$  which was the difference between observed streamflow ( $Q_B$ ) during changed periods and baseline. The fourth column showed the simulated streamflow ( $Q_S$ ) for the changed periods when using climate and calibrated parameter values from the baseline period.  $\Delta Q_H$  was the difference between  $Q_B$  and  $Q_S$  for changed periods, and  $\Delta Q_C$  was the difference between  $Q_S$  for changed period and  $Q_B$  of baseline.

The results showed that the average annual streamflow for 1971–2010 ( $12.3 \times 10^8 \text{ m}^3$ ) was less than that of the baseline period ( $18.3 \times 10^8 \text{ m}^3$ ), which means the recorded streamflow in the JRB markedly decreased over the past few decades. The total reduction  $\Delta Q$  in streamflow for the changed period of 1971–2010 (when compared to the baseline period) due to human activity and climate variability for JRB were  $4.6 \times 10^8$  and  $1.4 \times 10^8 \text{ m}^3$  for the TOPMODEL respectively, which was about 76.7 and 23.3 % of the total reduction. The corresponding reductions were  $4.7 \times 10^8 \text{ m}^3$  (78.3 %) and  $1.3 \times 10^8 \text{ m}^3$  (21.7 %) for the VIC model.

For the different periods of 1970s, 1980s, 1990s and 2000s, the reductions in streamflow due to human activity were  $5.6 \times 10^8 \text{ m}^3$  (81.2 % of the total change),  $3.8 \times 10^8 \text{ m}^3$  (95 % of the total change),  $3.0 \times 10^8 \text{ m}^3$  (52.6 % of the total change) and  $6.1 \times 10^8 \text{ m}^3$  (82.4 % of the total change) for TOPMODEL model and  $5.7 \times 10^8 \text{ m}^3$

5264

(82.6 % of the total change),  $4.5 \times 10^8 \text{ m}^3 \text{ mm}$  (112.5 % of the total change),  $3.2 \times 10^8 \text{ m}^3 \text{ mm}$  (56.1 % of the total change) and  $5.8 \times 10^8 \text{ m}^3 \text{ mm}$  (78.4 % of the total change) for VIC model respectively. Compared with the baseline period of 1960–1970, streamflow greatly decreased during 2001–2010. The change impacts (i.e.,  $\Delta Q_H$  and  $\Delta Q_C$ ) in 2001–2010 were about 77.4 and 22.6 % of the total reduction when averaged over the two methods.

#### 4.5 Climate elasticity model results

To assess the impacts of climate variability on streamflow, the climate elasticity of streamflow was calculated using Eqs. (3)–(4) based on the annual precipitation and annual potential evapotranspiration of the period 1971–2010. Table 6 summarized the annual precipitation ( $P$ ), potential evapotranspiration ( $E_0$ ), precipitation elasticity ( $\varepsilon_P$ ), evapotranspiration elasticity ( $\varepsilon_{E_0}$ ) of streamflow for different periods, and percentage change in streamflow results for different periods when using the elasticity-based approaches. The variation of  $\varepsilon_P$  was between 1.45 and 1.52, whilst the variation of  $\varepsilon_{E_0}$  was between  $-0.45$  and  $-0.52$ . As shown in Table 6, for the period of 1971–2010, the value of  $\varepsilon_P$  and  $\varepsilon_{E_0}$  obtained were 1.48 and  $-0.48$ , respectively. The results indicated that a 10 % decrease in precipitation would result in 14.8 % drop in streamflow, while a 10 % decrease in potential evapotranspiration would induce 4.8 % increase of streamflow. According to Eq. (3), with the calculated  $\varepsilon_P$  and  $\varepsilon_{E_0}$ , it can be estimated that the 6.1 mm decrease of precipitation in 1971–2010 may lessen the streamflow by 4.9 mm, meanwhile, the 7.3 mm increase in potential evapotranspiration may cause 5.1 mm decrease of streamflow.

The reductions in streamflow during 1971–2010 due to climate variability when using the Budyko framework method ranged between 7.5 and 29.9 % with a median of 19.3 % for the JRB. The maximum and minimum value of the aridity index ( $E_0/P$ , Willmott and Feddema, 1992) was 1.91 and 1.53 appeared in 1991–2000 and 1981–1990 respectively. Compared with 1960–1970 baseline period, reduction in  $\Delta Q$  for 1991–

5265

2000 and 1981–1990 was  $5.7 \times 10^8$  and  $4.0 \times 10^8 \text{ m}^3$ , with climate variability making the greatest and smallest contributions (i.e., 29.9 and 7.5 % see Table 6).

## 5 Discussion

### 5.1 Comparison of impact results from the three methods

In this paper, we used an elasticity-based analysis, TOPMODEL and VIC model to isolate hydrological impacts of human activity from that of climate variability. The climate elasticity method is relatively more simple and can be easily transplanted to other areas, and it gives a general streamflow change with less data and parameters (Ma et al., 2010). The hydrological modeling method, on the other hand, distinguishes more precisely streamflow change, such as monthly change or daily change. In this paper, the three methods were implemented independently at different time scales (climate elasticity method based on yearly scale, TOPMODEL based on monthly scale and Vic model hydrological simulation based on daily scale). For the whole JRB, the contribution ratios of climate variability in 1971–2010 were 23.3, 21.7 and 20 % from TOPMODEL, VIC hydrological modeling method and elasticity method respectively, and the mean contribution ratio is 21.7 %. The most significant climate variability impact was  $2.7 \times 10^8 \text{ m}^3$  (47.4 %),  $2.5 \times 10^8 \text{ m}^3$  (43.9 %) and  $1.7 \times 10^8 \text{ m}^3$  (29.9 %) for the TOMODEL, VIC model and elasticity based model, appearing in the 1990s. The most significant human activity impact was  $3.8 \times 10^8 \text{ m}^3$  (95 %),  $4.5 \times 10^8 \text{ m}^3$  (112.5 %) and  $3.7 \times 10^8 \text{ m}^3$  (92.4 %) for the TOMODEL, VIC model and elasticity based model, appearing in the 1980s. The analysis showed that the results from the two hydrological models were similar to those from the commonly used elasticity-based approach. We conclude that the three methods are in good agreement in terms of dominant contributor, i.e., human activity plays a more important role in the streamflow decrease than change in climate in the JRB. The main result of this research agrees with the findings of some other studies in Northwest China. Tang et al. (2013) used the climate

5266







- Chiew, F. H. S.: Estimation of rainfall elasticity of streamflow in Australia, *Hydrolog. Sci. J.*, 51, 613–625, 2006.
- Destouni, G., Jaramillo, F., and Prieto, C.: Hydroclimatic shifts driven by human water use for food and energy production, *Nature Climate Change*, 3, 213–217, doi:10.1038/nclimate1719, 2013.
- 5 Donohue, R. J., Roderick, M. L., and McVicar, T. R.: On the importance of including vegetation dynamics in Budyko's hydrological model, *Hydrol. Earth Syst. Sci.*, 11, 983–995, doi:10.5194/hess-11-983-2007, 2007.
- Donohue, R. J., Roderick, M. L., and McVicar, T. R.: Assessing the differences in sensitivities of runoff to changes in climatic conditions across a large basin, *J. Hydrol.*, 406, 234–244, doi:10.1016/j.jhydrol.2011.07.003, 2011.
- 10 Dooge, J. C., Bruen, M., and Parmentier, B.: A simple model for estimating the sensitivity of runoff to long-term changes in precipitation without a change in vegetation, *Adv. Water Resour.*, 23, 153–163, 1999.
- 15 Fu, B. P.: On the calculation of the evaporation from land surface, *Chinese Journal of Atmospheric Sciences*, 5, 23–31, 1981.
- Fu, B. P.: On the calculation of evaporation from land surface in mountainous areas, *Scientia Meteorologica Sinica*, 6, 328–335, 1996.
- Fu, G., Charles, S. P., and Chiew, F. S. H.: A two-parameter climate elasticity of streamflow index to assess climate change effects on annual streamflow, *Water Resour. Res.*, 43, W11419, doi:10.1029/2007WR005890, 2007.
- 20 Furusho, C., Chancibault, K., and Andrieu, H.: Adapting the coupled hydrological model ISBA-TOPMODEL to the long-term hydrological cycles of suburban rivers: evaluation and sensitivity analysis, *J. Hydrol.*, 485, 139–147, 2013.
- 25 Gao, H., Bohn, T. J., Podest, E., McDonald, K. C., and Lettenmaier, D. P.: On the causes of the shrinking of lake Chad, *Environ. Res. Lett.*, 6, 034021, doi:10.1088/1748-9326/6/3/034021, 2011.
- Gao, P., Geissen, V., Ritsema, C. J., Mu, X.-M., and Wang, F.: Impact of climate change and anthropogenic activities on stream flow and sediment discharge in the Wei River basin, China, *Hydrol. Earth Syst. Sci.*, 17, 961–972, doi:10.5194/hess-17-961-2013, 2013.
- 30 Grimson, R., Montroull, N., Saurral, R., Vasquez, P., and Camilloni, I.: Hydrological modelling of the Iberá Wetlands in southeastern South America, *J. Hydrol.*, 503, 47–54, doi:10.1016/j.jhydrol.2013.08.042, 2013.

5271

- Gumindoga, W., Rientjes, T. H. M., Haile, A. T., and Dube, T.: Predicting streamflow for land cover changes in the Upper Gilgel Abay River Basin, Ethiopia: a TOPMODEL based approach, *Phys. Chem. Earth*, doi:10.1016/j.pce.2014.11.012, online first, 2015.
- Hamed, K. H.: Trend detection in hydrologic data: the Mann–Kendall trend test under the scaling hypothesis, *J. Hydrol.*, 349, 350–363, 2008.
- 5 Li, H., Zhang, Y., Vaze, J., and Wang, B.: Separating effects of vegetation change and climate variability using hydrological modelling and sensitivity-based approaches, *J. Hydrol.*, 420–421, 403–418, 2012.
- Liang, X., Lettenmaier, D. P., Wood, E. F., and Burges, S. J.: A simple hydrologically based model of land surface water and energy fluxes for GSMs, *J. Geophys. Res.*, 99, 415–428, 1994.
- 10 Lin, S.-H., Liu, C.-M., Huang, W.-C., Lin, S.-S., Yen, T.-H., Wang, H.-R., Kuo, J.-T., and Lee, Y. C.: Developing a yearly warning index to assess the climatic impact on the water resources of Taiwan, a complex-terrain island, *J. Hydrol.*, 390, 13–22, 2010.
- 15 Liu, Q., Yang, Z., Cui, B., and Sun, T.: Temporal trends of hydro-climatic variables and runoff response to climatic variability and vegetation changes in the Yiluo River basin, China, *Hydrol. Process.*, 23, 3030–3039, 2009.
- Ma, H., Yang, D., Tan, S. K., Gao, B., and Fu, Q.: Impact of climate variability and human activity on streamflow decrease in the Miyun Reservoir catchment, *J. Hydrol.*, 389, 317–324, 2010.
- 20 Milly, P. C. D.: An analytic solution of the stochastic storage problem applicable to soil water, *Water Resour. Res.*, 29, 3755–3758, 1993.
- Milly, P. C. D. and Dunne, K. A.: Macroscale water fluxes 2. Water and energy supply control of their inter-annual variability, *Water Resour. Res.*, 38, 241–249, 2002.
- Notebaert, B., Verstraeten, G., Ward, P., Renssen, H., and Van Rompaey, A.: Modeling the sensitivity of sediment and water runoff dynamics to Holocene climate and land use changes at the catchment scale, *Geomorphology*, 126, 18–31, 2011.
- 25 Petchprayoon, P., Blanken, P. D., Ekkawatpanit, C., and Husseinc, K.: Hydrological impacts of land use/land cover change in a large river basin in central–northern Thailand, *Int. J. Climatol.*, 30, 1917–1930, 2010.
- 30 Potter, N. J. and Chiew, F. H. S.: An investigation into changes in climate characteristics causing the recent very low runoff in the southern Murray–Darling Basin using rainfall–runoff models, *Water Resour. Res.*, 47, W00G10, doi:10.1029/2010WR010333, 2011.

5272



**Table 1.** Statistical values of streamflow and precipitation in JRB.

Feature	Mean (mm)	Maximum		Minimum		Extremes ratio	Variation coefficient $C_v$	Flood period (%)	Dry period (%)
		time	(mm)	time	(mm)				
Precipitation	514	1964	794	1997	343	2.31	0.20	64.21	6.15
Streamflow	37	1964	96	2009	16	5.96	0.43	59.17	17.57
Runoff coefficient	0.07	1964	0.12	2009	0.04	3.34	0.28	–	–
Flood runoff coefficient	0.06	1964	0.12	2007	0.03	3.86	0.33	–	–









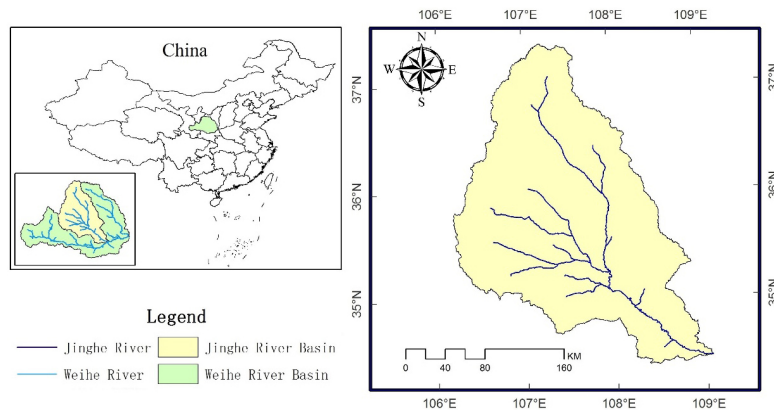


Figure 1. The location maps of (a) Weihe River basin; (b) Jinghe River basin.

5283

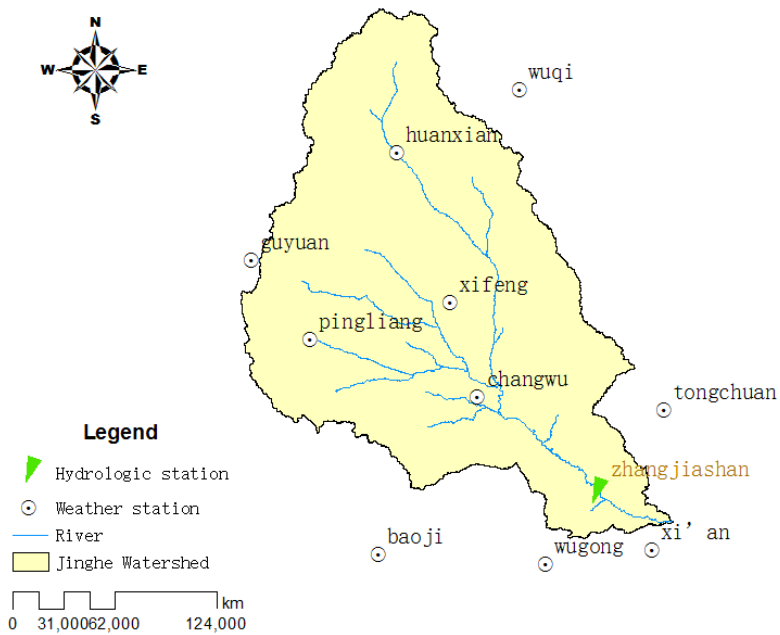
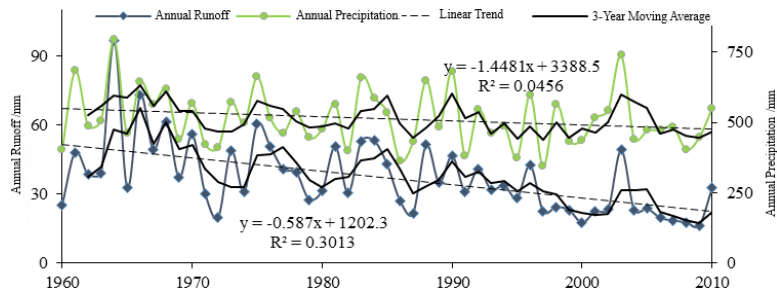


Figure 2. Location of hydrological and meteorological stations.

5284



**Figure 3.** Changes of annual streamflow and precipitation in JRB.

5285

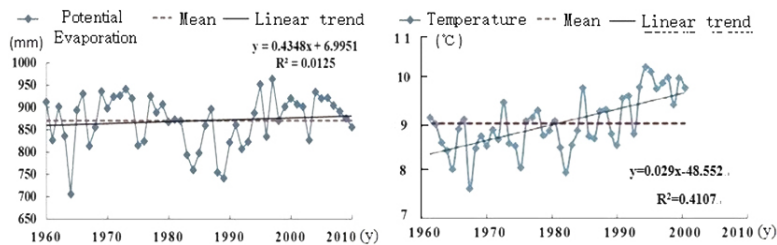


**Figure 4.** Changes of annual potential evaporation and temperature in JRB.

5286

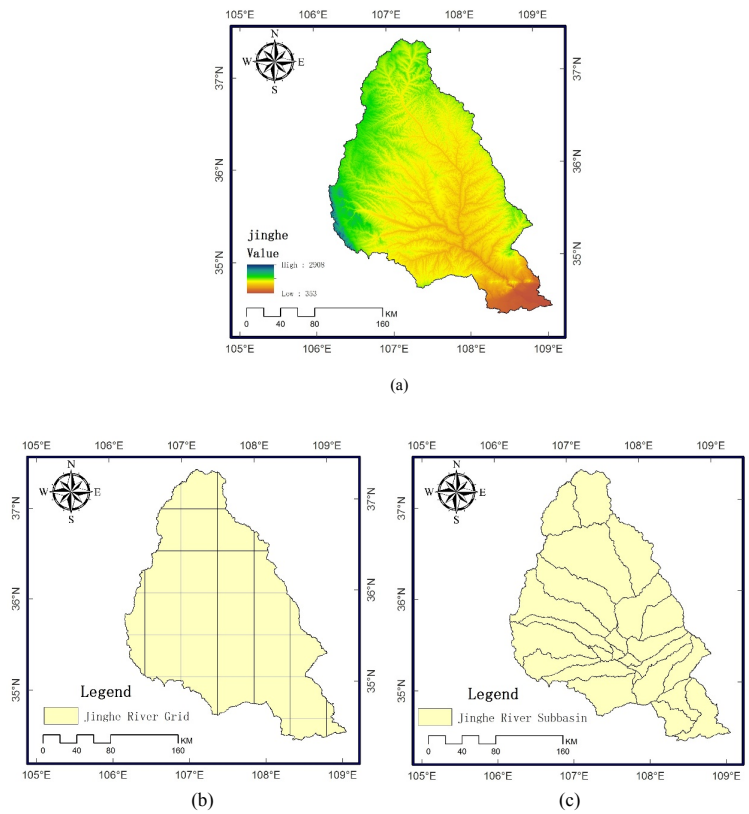


**Figure 5.** (a) Elevation maps of the study area at 40 m resolution. (b) Grid of VIC model. (c) Sub-basin of TOPMODEL.

5287

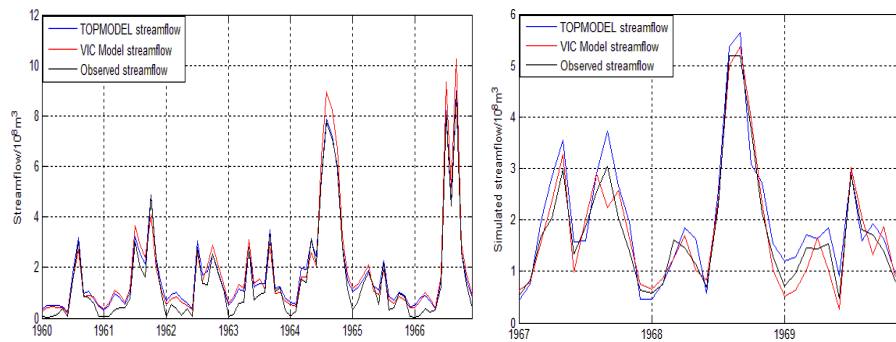


**Figure 6.** The simulated and observed streamflow for the calibration and validation period for TOPMODEL and VIC model (a) calibration period (b) validation period.

5288

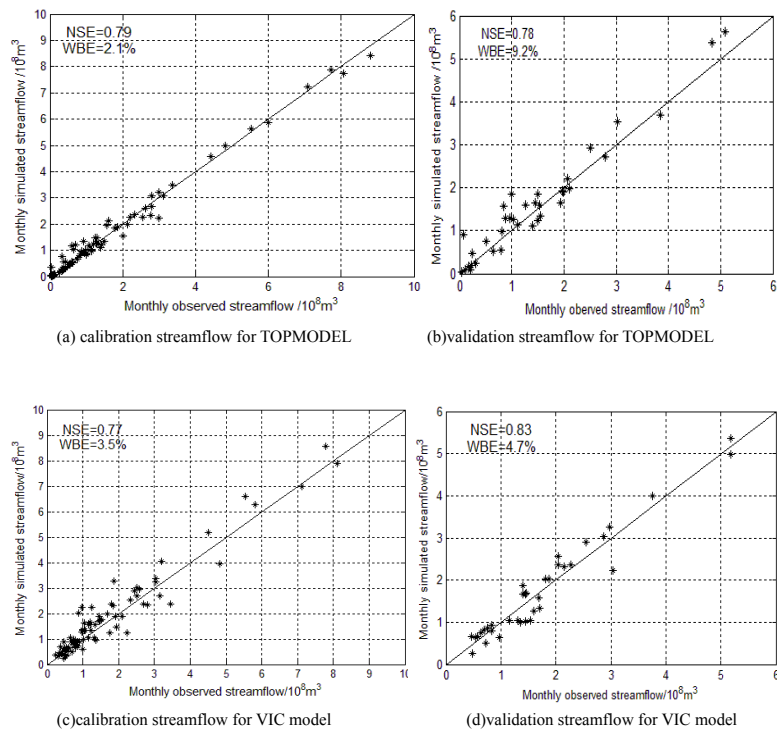


**Figure 7.** Comparison of observed and modelled monthly streamflow for calibration and validation periods.

5289

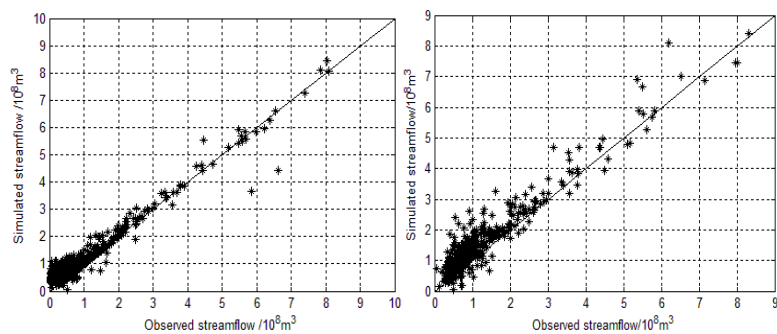


**Figure 8.** Comparison of observed and modelled monthly streamflow in 1971–2010. (a) TOPMODEL (b) VIC model.

5290

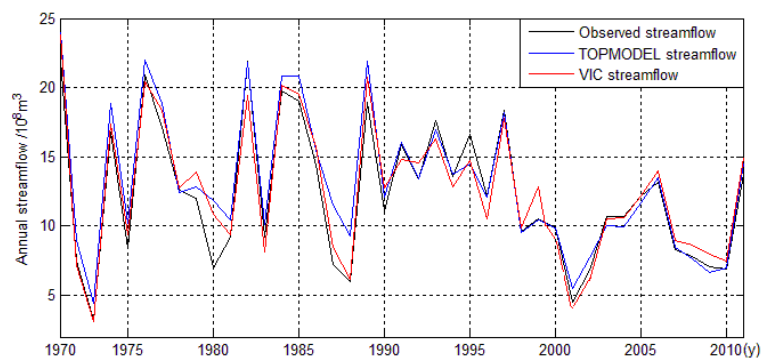


**Figure 9.** Time series of observed and model simulated annual streamflow for JRB for the entire modelling period.